
Supplementary Material for Submission #2869

Deep RGB-D Canonical Correlation Analysis For Sparse Depth Completion

Anonymous Author(s)

Affiliation

Address

email

1 Supplementary Material

2 1.1 Hyper-parameter Configuration

3 There are five main hyper-parameters in the CFCNet, including three weighting parameters in the
4 Equation (5) in the main paper, learning rate, and batch size. We carefully tune those hyper-parameters
5 for each experiment setting and record the configurations used for evaluation in this subsection.

- 6 • **KITTI dataset.** For KITTI dataset, we use 2 different weight settings, $(w_t, w_r, w_s) =$
7 $(0.5, 0.1, 0.1)$ and $(1, 0.1, 0)$. The batch size is set to be 7, and learning rate is 10^{-3} .
8 $(w_t, w_r, w_s) = (0.5, 0.1, 0.1)$ is used by the model generating Table 2. $(w_t, w_r, w_s) =$
9 $(1, 0.1, 0)$ is adopted to generate relative result in Table 3 in the paper.
- 10 • **Cityscape dataset.** For Cityscape dataset, We set $(w_t, w_r, w_s) = (1, 0.1, 0.1)$. The batch
11 size is set to be 12, and learning rate is 10^{-3} .
- 12 • **NYUv2 dataset.** For the model evaluated in Table 1, Table 4 and Table 5 in the paper, we
13 set $(w_t, w_r, w_s) = (1, 10, 1)$, batch size to be 4, and learning rate to be 10^{-3} .

14 1.2 Additional Ablation Studies

15 We first conduct the ablation study on KITTI dataset, using different loss combinations. We use the
16 official dataset split. We uniformly sample 100 points from the original LiDAR measurements of
17 training dataset as the sparse depth inputs. The whole LiDAR measurements are used as groundtruth
18 data. We show the performance of using different combinations of the proposed loss terms. The
19 results are in Table 1.

Table 1: Ablation study using different loss combinations on KITTI dataset.

| Loss Combination | MAE | RMSE | δ_1 | δ_2 | δ_3 |
|--|-------|-------|------------|------------|------------|
| L_{recon} | 1.649 | 3.752 | 91.1 | 97.1 | 99.0 |
| $L_{trans} + L_{recon}$ | 1.638 | 3.722 | 91.2 | 97.1 | 99.0 |
| $L_{2D^2CCA} + L_{trans} + L_{recon}$ | 1.612 | 3.676 | 91.2 | 97.1 | 99.0 |
| $L_{2D^2CCA} + L_{trans} + L_{recon} + L_{smooth}$ | 1.615 | 3.733 | 91.2 | 97.2 | 99.0 |

20 We also conduct the same ablation study on the NYUv2 dataset. We use official dataset split. We
21 used stereo sparsifier to sample 100 points from the dense depth map as our sparse depth inputs. The
22 results are shown in Table 2.

Table 2: Ablation study using different loss combinations on NYUv2 dataset.

| Loss Combination | MAE | RMSE | δ_1 | δ_2 | δ_3 |
|--|-------|-------|------------|------------|------------|
| L_{recon} | 0.439 | 0.594 | 76.0 | 93.7 | 98.4 |
| $L_{trans} + L_{recon}$ | 0.440 | 0.598 | 76.8 | 93.8 | 98.3 |
| $L_{2D^2CCA} + L_{trans} + L_{recon}$ | 0.428 | 0.581 | 77.6 | 94.2 | 98.4 |
| $L_{2D^2CCA} + L_{trans} + L_{recon} + L_{smooth}$ | 0.426 | 0.580 | 77.5 | 94.1 | 98.4 |

23 Next, we conduct the ablation study with different sparsity on NYUv2 dataset. We use stereo sparsifier
 24 to sample from dense depth maps to create sparse depth data. We show how different sparsity could
 25 affect the predicted depth map quality. The results are in Table 3.

Table 3: Ablation study of different sample numbers on NYUv2 using stereo sparsifier.

| Sample# | MAE | RMSE | δ_1 | δ_2 | δ_3 |
|---------|-------|-------|------------|------------|------------|
| 50 | 0.547 | 0.715 | 65.5 | 90.1 | 97.4 |
| 100 | 0.426 | 0.580 | 77.5 | 94.1 | 98.4 |
| 200 | 0.385 | 0.531 | 80.9 | 95.1 | 98.7 |
| 500 | 0.342 | 0.476 | 83.0 | 96.1 | 99.0 |
| 1000 | 0.290 | 0.419 | 87.0 | 97.0 | 99.2 |
| 2000 | 0.242 | 0.352 | 91.3 | 98.2 | 99.6 |
| 5000 | 0.222 | 0.323 | 93.3 | 98.9 | 99.8 |
| 10000 | 0.151 | 0.231 | 96.6 | 99.5 | 99.9 |

26 1.3 Additional Visual Results

27 We showed several additional visual results. Results of using the stereo sparsifier on NYUv2 dataset
 28 are shown in Figure 1. Results of using the ORB sparsifier on NYUv2 dataset are shown in Figure 2.
 29 Results of using the ORB sparsifier on ICL-NUIM are shown in Figure 3. We also make a video clip
 30 of the depth completion using our CFCNet on KITTI dataset in the other file.

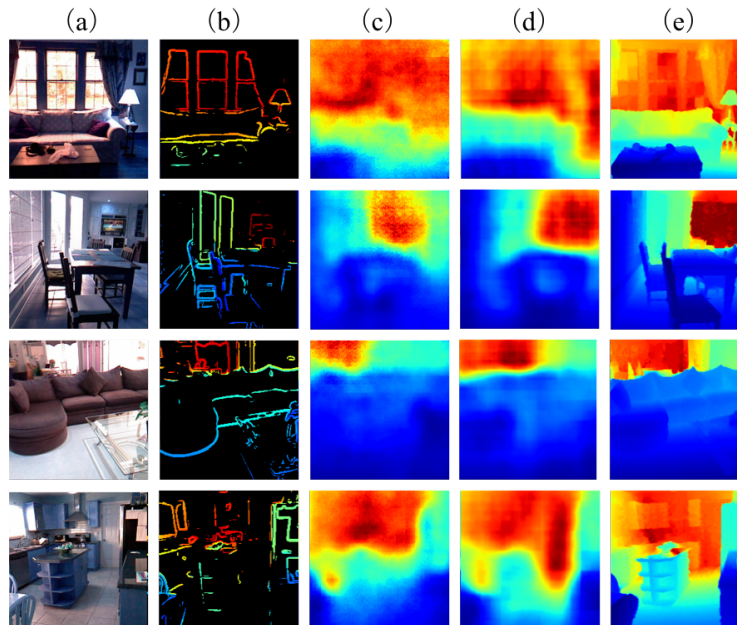


Figure 1: Visual results on NYUv2 dataset using stereo sparsifier. (a) The RGB images (b) 5000 points sparse depth. (c) Results from [1]. (d) Our completed depth maps. (e) Groundtruth dense depth maps.

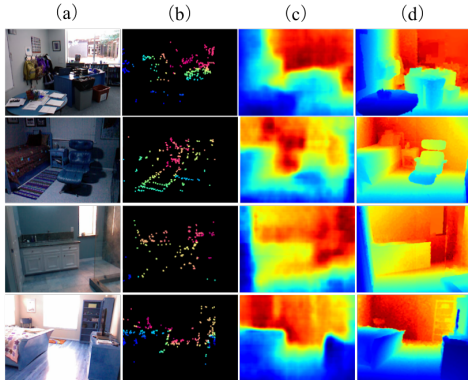


Figure 2: Visual results on NYUv2 dataset using ORB sparsifier. (a) The RGB images (b) ORB sparse depth. (c) Our completed depth maps. (d) Groundtruth dense depth maps.

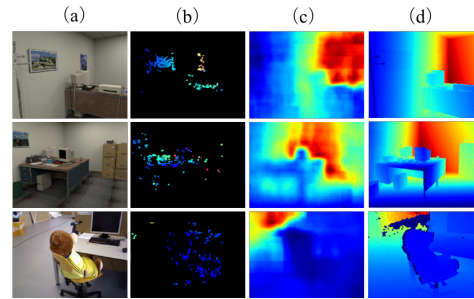


Figure 3: Sample results of cross-dataset testing on ICL-NUIM dataset and TUM dataset using ORB sparsifier. Tested model is trained on NYUv2 dataset and is the same model used in Figure 2. (a) The RGB images (b) ORB sparse depth. (c) Our completed depth maps. (d) Groundtruth dense depth maps

31 **References**

32 [1] Fangchang Ma and Sertac Karaman, “Sparse-to-dense: Depth prediction from sparse depth
 33 samples and a single image,” in *IEEE International Conference on Robotics and Automation*
 34 (*ICRA*), 2018.